

PAPER

# Atomically thin $\alpha$ - $\text{In}_2\text{Se}_3$ : an emergent two-dimensional room temperature ferroelectric semiconductor

To cite this article: Yue Li *et al* 2019 *J. Semicond.* **40** 061002

View the [article online](#) for updates and enhancements.

## Recent citations

- [Ferroelectric field effect transistors: Progress and perspective](#)  
Jae Young Kim *et al*
- [Sm doped BiFeO<sub>3</sub> nanofibers for improved photovoltaic devices](#)  
Junying Zhang *et al*
- [Nd-Cr co-doped BiFeO<sub>3</sub> thin films for photovoltaic devices with enhanced photovoltaic performance](#)  
Junying Zhang *et al*

# Atomically thin $\alpha$ - $\text{In}_2\text{Se}_3$ : an emergent two-dimensional room temperature ferroelectric semiconductor

Yue Li<sup>1,2</sup>, Ming Gong<sup>3,4</sup>, and Hualing Zeng<sup>1,2,†</sup>

<sup>1</sup>International Center for Quantum Design of Functional Materials (ICQD), Hefei National Laboratory for Physical Science at the Microscale, University of Science and Technology of China, Hefei 230026, China

<sup>2</sup>Key Laboratory of Strongly-Coupled Quantum Matter Physics, Chinese Academy of Sciences, Department of Physics, University of Science and Technology of China, Hefei 230026, China

<sup>3</sup>CAS Key Laboratory of Quantum Information, University of Science and Technology of China, Hefei 230026, China

<sup>4</sup>Synergetic Innovation Center of Quantum Information and Quantum Physics, University of Science and Technology of China, Hefei 230026, China

**Abstract:** Room temperature ferroelectric thin films are the key element of high-density nonvolatile memories in modern electronics. However, with the further miniaturization of the electronic devices beyond the Moore's law, conventional ferroelectrics suffer great challenge arising from the critical thickness effect, where the ferroelectricity is unstable if the film thickness is reduced to nanometer or single atomic layer limit. Two-dimensional (2D) materials, thanks to their stable layered structure, saturate interfacial chemistry, weak interlayer couplings, and the benefit of preparing stable ultra-thin film at 2D limit, are promising for exploring 2D ferroelectricity and related device applications. Therefore, it provides an effective approach to overcome the limitation in conventional ferroelectrics with the study of 2D ferroelectricity in van der Waals (vdW) materials. In this review article, we briefly introduce recent progresses on 2D ferroelectricity in layered vdW materials. We will highlight the study on atomically thin  $\alpha$ - $\text{In}_2\text{Se}_3$ , which is an emergent ferroelectric semiconductor with the coupled in-plane and out-of-plane ferroelectricity. Furthermore, two prototype ferroelectric devices based on ferroelectric  $\alpha$ - $\text{In}_2\text{Se}_3$  will also be reviewed.

**Key words:** electric polarization; 2D materials; 2D ferroelectrics

**Citation:** Y Li, M Gong, and H L Zeng, atomically thin  $\alpha$ - $\text{In}_2\text{Se}_3$ : an emergent two-dimensional room temperature ferroelectric semiconductor[J]. *J. Semicond.*, 2019, 40(6), 061002. <http://doi.org/10.1088/1674-4926/40/6/061002>

## 1. Introduction

Owning the switchable and non-volatile electric polarizations at room temperature, conventional ferroelectrics, such as complex perovskite oxides, have broad applications in electronics, including high energy density capacitor<sup>[1]</sup>, tunable diode<sup>[2]</sup>, ferroelectric tunneling junction (FTJ)<sup>[3]</sup>, and ferroelectric field-effect transistors (FeFET)<sup>[4]</sup>. With the further miniaturization of electronic devices beyond the Moore's law, there is a need to explore ferroelectric thin films with nanometer thickness. However, due to the imperfect charge screening, local chemical environment, defects, and misfit strain at the interface, there is depolarization field arising in ultra-thin ferroelectrics, which leads to the so-called critical size effect<sup>[5–9]</sup>. The electric polarizations of conventional ferroelectrics will reduce or even disappear when the thickness reaches to the single atomic layer limit. As a consequence, their application in modern electronics is strongly hindered. In parallel, since the rise of graphene, the family of two-dimensional (2D) materials has been greatly expanded with members owning numerous novel physical properties such as superconductivity<sup>[10]</sup>, charge density wave<sup>[11]</sup>, valley polarization<sup>[12]</sup>, and exotic magnetism<sup>[13]</sup>. These van der Waals (vdW) materials have saturated interface chemical environment, weak interaction between the layers and the

benefit of easily preparing stable atomically thin slabs, which offer a novel platform to study some emerging phenomena that have never been observed in their bulk form counterpart. Therefore, it offers a feasible way to explore ferroelectricity at atomic scale in 2D materials, especially for the out-of-plane electric polarizations, which is more important than the in-plane electric polarization from the technological perspective.

In the early days of the research on vdW materials, 2D ferroelectricity is lack of attention with rare findings. The reason is that when the thickness is reduced to nanometer scale, the competition between crystal structure stability and the long-range ordering of electric dipoles will become significant. Thus, for a long time, it is hard to get stable crystal phase with switchable electric polarizations in vdW materials under ambient conditions. As ferroelectrics, the prerequisite is the inversion symmetry breaking in structure. For most of the commonly studied 2D materials, taking graphene as a typical example<sup>[14]</sup>, the centrosymmetric lattice naturally rules out the possibility of being ferroelectric. Even in  $2\text{H-MoS}_2$ <sup>[15, 16]</sup>, where the inversion symmetry is explicitly broken in its monolayer structure, the presence of the mirror symmetry along its middle plane of metal Mo atoms makes it keeping symmetric Mo-S chemical bonds in the out-of-plane direction, resulting void electric dipoles. Given these facts, seeking 2D ferroelectricity in vdW materials is of challenges but of great values.

The 2D nature of vdW materials allows to explore ferroelectricity in both the in-plane and out-of-plane directions. The in-

Correspondence to: H L Zeng, [hlzeng@ustc.edu.cn](mailto:hlzeng@ustc.edu.cn)

Received 31 MARCH 2019; Revised 30 APRIL 2019.

©2019 Chinese Institute of Electronics

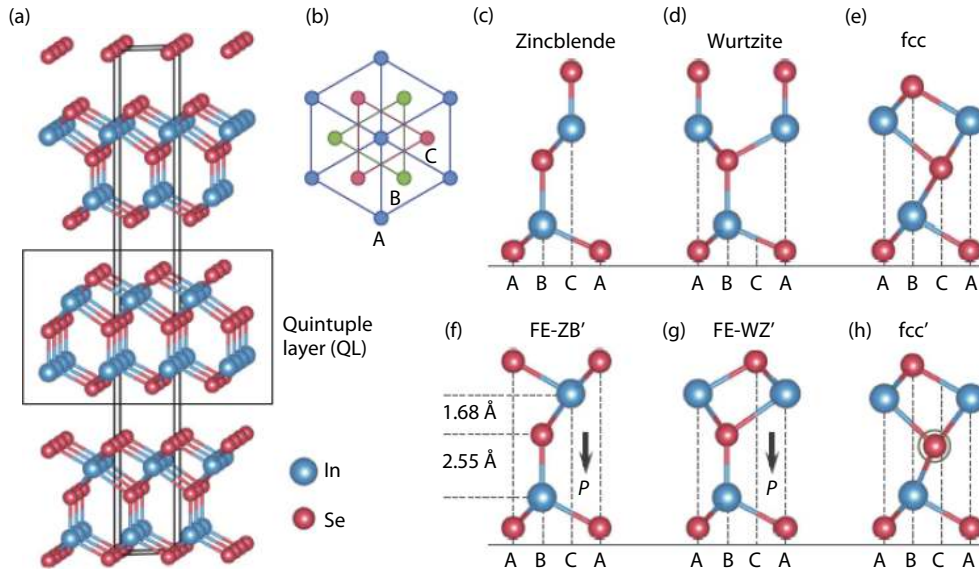


Fig. 1. (Color online) Layered structures of  $\text{In}_2\text{Se}_3$ . (a) Three-dimensional crystal structure of layered  $\text{In}_2\text{Se}_3$ , with the In atoms in blue and Se atoms in red, and a quintuple layer (QL) is indicated by the black dashed square. (b) Top view of the system along the vertical direction. Each atomic layer in a QL contains only one elemental species, with the atoms arranged in one of the triangular lattices A, B or C as illustrated. (c–h) Side views of several representative structures of one QL  $\text{In}_2\text{Se}_3$ , among which the (c) to (e) structures are derived from the zincblende, wurtzite and fcc crystals, respectively. In (f), the interlayer spacings between the central Se layer and the two neighboring In layers are displayed. The black arrows in (f) and (g) indicate the directions of the spontaneous electric polarization ( $P$ ) in the FE-ZB' and FE-WZ' structures, respectively. The FE-ZB' and FE-WZ' structures in (f) and (g) are identified as  $\alpha$  phase, while the metastable structure fcc and fcc' in (e) and (h) are identified as  $\beta$  phase. (Courtesy of Ref. [20])

plane vdW ferroelectrics provide a platform to study domain physics at 2D limit, while the out-of-plane ferroelectric polarizations lay down the fundamental for device applications. In recent years, several candidates of 2D ferroelectrics have been theoretically predicated and verified experimentally. The first example is the layered  $\text{CuInP}_2\text{S}_6$ . In 2015, Belianinov *et al.*[17] reported the observation of room-temperature out-of-plane ferroelectricity in bulk  $\text{CuInP}_2\text{S}_6$  with film thickness more than 100 nm. The electric polarization stemmed from the off-center ordering of the Cu and In cations in each unit cell with its polar axis along the vertical direction relative to the 2D plane. Although the collinear two-sublattice structure of  $\text{CuInP}_2\text{S}_6$  makes it a ferrielectric system, this finding also inspires further exploration on 2D ferroelectrics. Later in 2016, Liu *et al.*[18] observed the out-of-plane electric polarization in few-layer  $\text{CuInP}_2\text{S}_6$  with much thinner thickness of 4 nm under ambient conditions. Utilizing the second harmonic generation (SHG) technique, they clearly showed that the phase transition temperature ( $T_c$ ) from the ferroelectric phase to the paraelectric phase is 320 K, which is slightly higher than the room temperature. This is crucial for their practical device application. At the same time, Chang *et al.*[19] from Tsinghua University experimentally reported the first 2D ferroelectric with single atomic layer thickness. They studied the monolayer SnTe with distorted lattice at cryogenic temperature and verified the in-plane ferroelectricity with evidences such as spontaneous domains and electric polarization induced band bending. These pioneering findings open up the route towards 2D ferroelectricity with vdW materials. However, for layered SnTe, the nature as an in-plane ferroelectric strongly hinders its application in practical device application, while for  $\text{CuInP}_2\text{S}_6$ , it is ferrielectric, resulting relatively weak saturated electric polarizations. From the past researches on ferroelectricity, as a consensus, their prac-

tical application relies on the technically more important out-of-plane electric polarization, high  $T_c$  and simple lattice structure for material realization. Based on these requirements, very recently Ding *et al.*[20] predicted the intrinsic room-temperature 2D ferroelectricity with intercorrelated in-plane and out-of-plane electric polarization in the 2D semiconducting  $\alpha\text{-In}_2\text{Se}_3$ . Stimulated by this unprecedented inter-locking of electric dipoles in  $\alpha\text{-In}_2\text{Se}_3$ , intense experimental efforts were devoted with various techniques[21–28]. Clear ferroelectric domains, ferroelectric hysteresis loop and piezoelectricity have been observed in ultrathin samples with the thickness down to 2D limit[23, 26]. Besides, several practical device applications based on the few layer  $\alpha\text{-In}_2\text{Se}_3$  including switchable ferroelectric diode[24], FeFETs[29], and ferroelectric semiconductor FET (FeSFET)[30] were demonstrated. These breakthroughs point to the possibility of stable ferroelectric phase in layered vdW materials.

In view of the rapid growing research interest in the 2D ferroelectricity of  $\alpha\text{-In}_2\text{Se}_3$ , we review some recent relevant progresses in this article. We begin with the introduction of the crystal structure of  $\alpha\text{-In}_2\text{Se}_3$  and the corresponding ferroelectricity. The experimental verifications of the in-plane and out-of-plane electric polarizations in ultra-thin  $\alpha\text{-In}_2\text{Se}_3$  will be highlighted. Finally, we present two prototypes of ferroelectric devices to demonstrate the potential device application of 2D ferroelectric  $\alpha\text{-In}_2\text{Se}_3$ .

## 2. Crystal structure of layered $\alpha\text{-In}_2\text{Se}_3$

Layered  $\text{In}_2\text{Se}_3$  is an available 2D semiconductor with remarkable optical and electrical properties[31–33]. It has long been studied in the application of photo sensors and phase-change memories[34–36]. Previous studies have found that the phases of  $\text{In}_2\text{Se}_3$  are very rich. In addition to the  $\alpha$  phase, there

exists crystal structures with different lattice constants, which are labeled as  $\beta$ ,  $\gamma$  or  $\delta$  phase. In all these phases, the  $\alpha$ - $\text{In}_2\text{Se}_3$  is recognized as the most stable layered structure at room temperature. As shown in Fig. 1, its single layer is composed of alternating Se or In atomic layer via covalent bonds, constituting a Se–In–Se–In–Se quintuple layer (QL). These QLs are vertically stacked via the weak van der Waals force. However, the identification of the crystal structure for  $\alpha$  phase is highly controversial at early stage<sup>[31–35, 37–39]</sup>, which is due to the small energy barrier in structure stability between the  $\alpha$  and  $\beta$  phase.

To clarify the crystal structure of  $\text{In}_2\text{Se}_3$ , Ding *et al.*<sup>[20]</sup> has performed detailed numerical calculations with density functional theory (DFT). They examined the possible atomic arrangements in layered  $\text{In}_2\text{Se}_3$ , and obtained two lattice structures with lowest total energy in thermodynamics. As shown in Figs. 1(f) and 1(g), the FE-ZB' and the FE-WZ' structures were identified as ground states, which belonged to  $\alpha$  phase. From the top view of its crystal structure, there are three positions marked as A, B, and C (represent one corner of the triangular lattices in Fig. 1(b)) that can be occupied by Se or In atoms. Along the out-of-plane direction, the atoms of a given QL in FE-ZB' and FE-WZ' structure are arranged with ABBCA and ABBAC sequence respectively. For the ABCAB structure (Fig. 1(e)), it is identified as  $\beta$  phase, which is metastable at room temperature. With the confirmation of its crystal structure, they predicted the emergence of 2D ferroelectricity in  $\alpha$ - $\text{In}_2\text{Se}_3$ , which was attributed to the subtle atomic configuration of the central Se atoms. Taking the FE-ZB' structure as an example, in each QL, the Se and In atoms in the lower three Se–In–Se atomic layers form a regular tetrahedral structure, while the in the upper Se–In–Se layers they form the octahedral structure. Thus, the Se atoms in the middle layer are in different chemical environments with respect to its neighboring layers. This breaks the central inversion symmetry thereby produces the electric polarizations along both the out-of-plane and in-plane direction. Moreover, in  $\alpha$ - $\text{In}_2\text{Se}_3$ , the in-plane and out-of-plane electric dipoles are inherently coupled, which not only provides a novel approach of electric polarization manipulation with external electric field but also helps the stabilization of the out-of-plane electric polarizations against the depolarization electric field in ultrathin samples. In contrast, the  $\beta$  phase of  $\text{In}_2\text{Se}_3$  presented in Fig. 1(e) follows the ABCAB layer sequence with the central inversion symmetry, which forbids the spontaneous formation of net electric polarizations. Meanwhile, due to the structural phase transition, the phonon modes of  $\alpha$  and  $\beta$  phases of  $\text{In}_2\text{Se}_3$  were predicted to have distinct features, such as the softening of A1 phonon mode in the ferroelectric phase. These Raman modes can be utilized as an effective tool to identify the  $\alpha$ - $\text{In}_2\text{Se}_3$  in following experimental studies, including the results in our group<sup>[21–22, 24, 25, 29]</sup>.

As for ferroelectrics, one important signature is the switchable electric polarization with external stimulus such as electric field. For  $\alpha$ - $\text{In}_2\text{Se}_3$ , intuitively, the degenerate polarization states with opposite polarity can be achieved by in-plane 180° rotation of a single QL without changing the crystal structure and symmetry. It has been theoretically suggested that the transformation of these two polarization states is kinetically feasible<sup>[20]</sup>. The flipping process is proposed as "three-step cooperated polarization inversion process", where the electron polarization reversion is achieved by the metastable fcc' structure ( $\beta$  phase) as the intermediate transition state. The en-

ergy barrier for polarization flipping is only 0.066 eV per unit cell, which is comparable with that in conventional ferroelectric material  $\text{PbTiO}_3$  (0.07 eV/ unit cell). This feasible polarization flipping process in  $\alpha$ - $\text{In}_2\text{Se}_3$  further evidence its ferroelectric nature.

### 3. Experimental verification of coupled ferroelectricity in 2D $\alpha$ - $\text{In}_2\text{Se}_3$

Inspired by the previous theoretical prediction, several groups have aimed to experimentally verify the room temperature ferroelectricity in  $\alpha$ -phase  $\text{In}_2\text{Se}_3$ <sup>[21–26, 28]</sup>. Ferroelectrics naturally have the piezoelectric effect, in which deformation of the crystals can be realized by an external electric field. Therefore, the detection of ferroelectricity in vdW materials can be realized via surface sensitive techniques such as Piezo force microscopy (PFM). In most of recent studies on the 2D ferroelectricity in  $\alpha$ - $\text{In}_2\text{Se}_3$ , PFM was chosen as the versatile tool. Fig. 2 shows the typical PFM study on ultra-thin  $\alpha$ - $\text{In}_2\text{Se}_3$  with thickness about 20 nm under ambient condition<sup>[24]</sup>. The samples were mechanically exfoliated from bulk and post transferred to conductive substrate such as heavily doped Si or Au. Clear out-of-plane spontaneous electric polarizations were visualized through the contrasted PFM phase image as shown in Fig. 2(b). The phase difference between adjacent ferroelectric domains was found to be 180°, indicating that there were anti-parallel electric dipoles (Fig. 2(c)) in the out-of-plane direction. In the single poling measurement, the butterfly-like ferroelectric hysteresis is observed in the out-of-plane PFM amplitude (see Fig. 2(d)), and the transition between the two different ferroelectric states can also be driven by an external electric field, with two different critical field strengths during forward and backward sweeping (see Fig. 2(e)). These results show that the electric polarization could be flipped under external electric field. The coercive field ( $E_c$ ) of  $\alpha$ - $\text{In}_2\text{Se}_3$  was found to be about 200 kV/cm<sup>[24]</sup>, which was much lower than that of layered ferroelectric  $\text{CuInP}_2\text{S}_6$  (700 kV/cm)<sup>[18]</sup>. The relatively low  $E_c$  benefits the low operating power ferroelectric device based on  $\alpha$ - $\text{In}_2\text{Se}_3$ . Other important features of ferroelectrics include the domain engineering and the retention of electric polarizations. In order to verify these features, artificially creating the ferroelectric domain structure with the box-in-box pattern (Fig. 2(f)) has been tested in  $\alpha$ - $\text{In}_2\text{Se}_3$ . In detail, a square area of  $1 \times 1 \mu\text{m}^2$  is controllably written with positive bias via the PFM tip to establish the downward polarization. After that, the negative sample/tip bias is applied in the center  $0.5 \times 0.5 \mu\text{m}^2$  area to reverse or erase the polarization. As a result of the ferroelectric nature of  $\alpha$ - $\text{In}_2\text{Se}_3$ , an artificial domain structure with the box-in-box pattern is created. It is found that artificial ferroelectric domain could sustain more than 24 h under ambient condition<sup>[24]</sup>.

Another method to study the 2D ferroelectricity in vdW materials is the optical SHG technique, which is a direct probe of the lattice inversion symmetry breaking. With this technique, Xiao *et al.*<sup>[25]</sup> has verified the out-of-plane and in-plane electric dipole inter-locking in  $\alpha$ - $\text{In}_2\text{Se}_3$ , which is consistent with previous PFM study<sup>[22]</sup>. The rotation of in-plane electric dipole could be achieved by an out-of-plane electric field, which demonstrates the inherent locking of these two orthogonal polarizations. As shown in Fig. 3, in a 3-nm-thick sample with confirmed electric polarization, they first artificially construct the box-in-box domain in the out-of-plane direction with the PFM tip. In their SHG measurements, the normal incidence set-up is



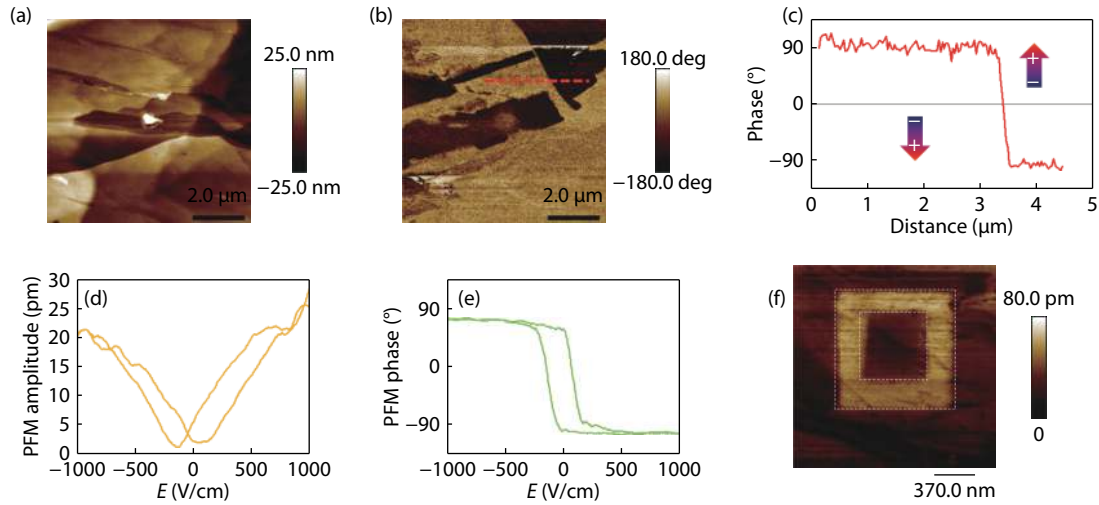


Fig. 2. (Color online) Ferroelectricity of  $\alpha$ - $\text{In}_2\text{Se}_3$  thin layers. (a) The surface topography of  $\alpha$ - $\text{In}_2\text{Se}_3$  thin layers ( $\sim 20$  nm) on the heavily doped Si substrate. The scale bar is  $2\ \mu\text{m}$ . (b) The corresponding PFM phase image in the out-of-plane direction, showing clear ferroelectric domains. (c) The phase profile of different ferroelectric domains as sketched by the red dashed line in (b). A phase contrast of  $180^\circ$  is observed, which indicates the antiparallel directions of out-of-plane electric polarization between the adjacent domains. The arrows indicate the directions of electric polarization. (d) PFM amplitude and (e) PFM phase hysteresis loop measured from  $\alpha$ - $\text{In}_2\text{Se}_3$  thin layers. (f) PFM amplitude image of domain engineering in  $\alpha$ - $\text{In}_2\text{Se}_3$  with a film thickness of 12 nm. The scale bar is  $370\ \text{nm}$ . (Courtesy of Ref. [24])

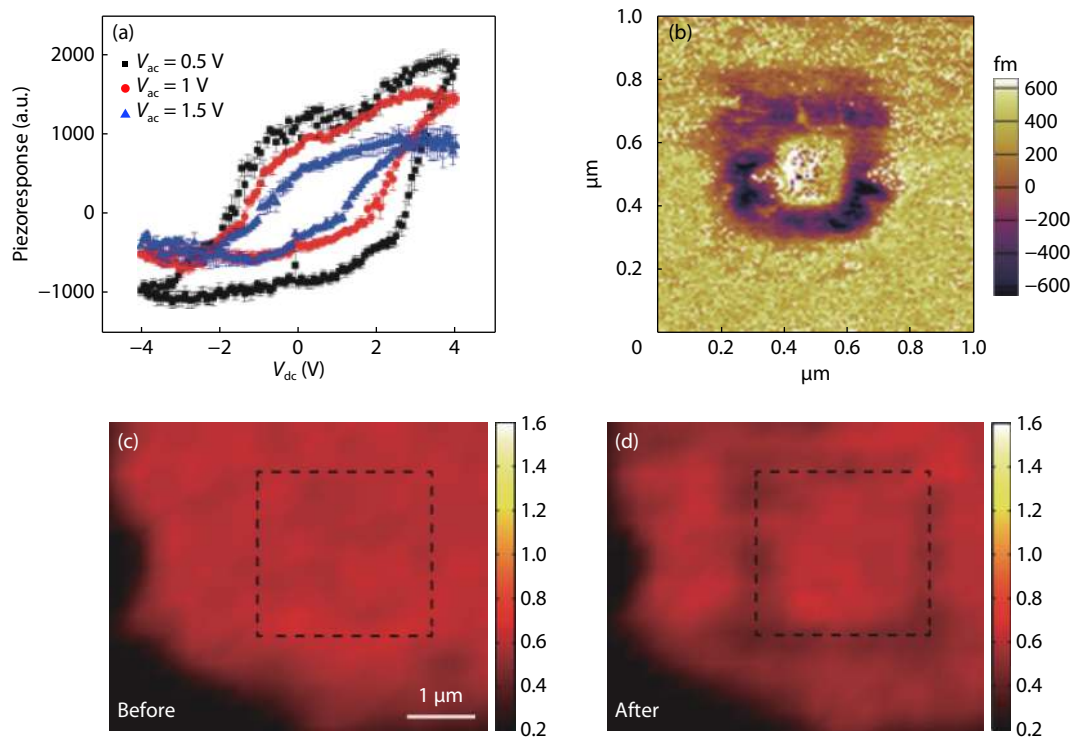


Fig. 3. (Color online) Electrically switching the out-of-plane ferroelectric polarization and corresponding in-plane atomic configuration through dipole locking. (a) The hysteresis of remnant out-of-plane polarization of a 3-nm-thick  $\text{In}_2\text{Se}_3$  crystal on conductive  $\text{SrRuO}_3$ , as a function of perpendicular poling voltage. Black, red, blue curves represent the normalized piezoresponse measured with  $V_{\text{ac}} = 0.5, 1, \text{ and } 1.5\ \text{V}$ , respectively. The collapse of the hysteresis loop is similar to the behavior of the conventional field-switchable ferroelectrics, but totally different from charging artifact of dielectrics. (b) Polarized domain patterned by electrically biased scanning probe and measured by PFM. The inner box corresponds to positive applied voltage ( $+6\ \text{V}$ ) with positive piezoresponse while the outer box to negative voltage ( $-6\ \text{V}$ ) with negative piezoresponse. (c) SHG intensity mapping on another trilayer  $\text{In}_2\text{Se}_3$  sample before PFM reversed poling. The area enclosed by dashed line was then scanning by a negatively biased AFM tip. The color bar is in linear scale with arbitrary unit. (d) SHG mapping after the electrical reversed poling. It shows dark lines at the boundary of the patterned area resulting from destructive interference, which indicates the reversal of in-plane crystal orientation and corresponding nonlinear optical polarization after reversed electrical poling. (Courtesy of Ref. [25])

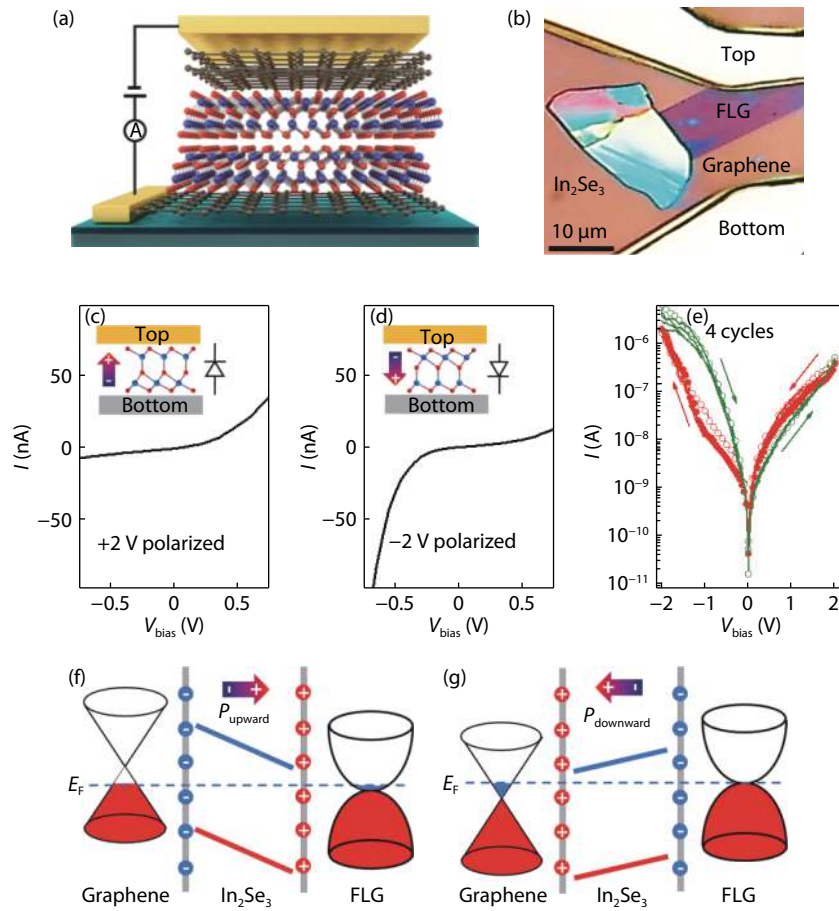


Fig. 4. (Color online) Switchable ferroelectric diode based on  $\alpha$ - $\text{In}_2\text{Se}_3$  thin layers. (a) Schematic and (b) optical image of the device. (c) and (d)  $I$ - $V$  curves of the ferroelectric diode with switchable rectifying behavior. (e)  $I$ - $V$  curves measured under high DC bias, showing clear hysteresis characteristics. The arrows indicate the voltage sweeping sequence. (f) and (g) Schematic of energy band diagrams of the graphene/ $\text{In}_2\text{Se}_3$  heterostructure, illustrating the evolution of the Schottky barrier in the polarized state of the ferroelectric. The positive and negative charges on the vertical grey lines stand for the polarization charges on the top and bottom sides of the  $\alpha$ - $\text{In}_2\text{Se}_3$  thin layer. The screening charges are visualized in the graphene/FLG electrodes. (Courtesy of Ref. [24])

chosen, which is only sensitive to the in-plane electric polarization. By comparing the SHG mappings before and after the out-of-plane bias poling (Figs. 3(c) and 3(d)), clear dark lines (less SHG intensity) correspond to the boundaries of the patterned area by PFM tip bias. This observation can be understood as the destructive optical interference arising from the reversal of the in-plane nonlinear optical polarization and corresponding in-plane lattice asymmetry. These findings clearly demonstrate the interlocking of the out-of-plane and in-plane electric dipoles in 2D  $\alpha$ - $\text{In}_2\text{Se}_3$ . Moreover, the temperature-dependent SHG is also studied, which show that the SHG intensity is robust and is almost independent of temperature in a wide range of temperature range up to 500 K. The transition from the ferroelectric phase to paraelectric phase happens at about 700 K, beyond which a sharp decrease of SHG signal can be found due to the recovery of structural inversion symmetry. These results confirm that the  $T_c$  for ferroelectric  $\alpha$ - $\text{In}_2\text{Se}_3$  is much higher than that of the other 2D ferroelectrics such as SnTe and  $\text{CuInP}_2\text{S}_6$ , laying the fundamental basis for its practical device application.

#### 4. Ferroelectric device application of atomically thin $\alpha$ - $\text{In}_2\text{Se}_3$

The vacuum potential difference between the top and bot-

tom surfaces of a given  $\alpha$ - $\text{In}_2\text{Se}_3$  QL can be as high as 1.4 eV<sup>[20]</sup>. The sign of this potential difference can be controlled by the direction of polarization. Therefore, when the 2D ferroelectric  $\alpha$ - $\text{In}_2\text{Se}_3$  is artificially combined with other vdW materials to form multi-layer vdW heterojunction, the physical properties of the entire heterojunction will be manipulated by the electric polarization. Tuning the properties of the ferroelectric heterojunction as a whole can be simply achieved by reversing the polarity of the ferroelectrics with an external electric field. With this feature, it is convenient to develop multifunctional ferroelectric device with 2D ferroelectrics.

We firstly introduce the ferroelectric diode application based on 2D  $\alpha$ - $\text{In}_2\text{Se}_3$ . With the out-of-plane ferroelectricity of  $\alpha$ - $\text{In}_2\text{Se}_3$ , a polarity switchable ferroelectric diode with the vertical few-layer graphene/ $\alpha$ - $\text{In}_2\text{Se}_3$ /graphene heterojunction is proposed and experimentally demonstrated<sup>[24]</sup>. Figs. 4(a) and 4(b) show the device structure and optical image of the proposed ferroelectric diode, in which the thickness of the ferroelectric layer  $\alpha$ - $\text{In}_2\text{Se}_3$  is as thin as 5 nm. Graphene and few-layer graphene serve as the bottom and top electrodes, respectively. By comparing work functions of  $\alpha$ - $\text{In}_2\text{Se}_3$ , monolayer graphene (p-type) and few-layer graphene (intrinsic), the Schottky barrier at bottom graphene/ $\alpha$ - $\text{In}_2\text{Se}_3$  is found to be higher than  $\alpha$ - $\text{In}_2\text{Se}_3$ /top graphene. Therefore, the initial state of the di-

ode is in the forward direction, thus the current flows from  $\alpha$ - $\text{In}_2\text{Se}_3$  to the FLG. When the device is polarized with +2 V pulse voltage, as shown in Fig. 4(c), it shows an enhanced forward rectifying behavior. However, in the case of -2 V polarized state, the device functions as a backward diode, allowing the current conduction from  $\alpha$ - $\text{In}_2\text{Se}_3$  to bottom graphene (Fig. 4(d)). This polarity-controlled rectification effect could be understood through the band structure of the device (Figs. 4(f) and 4(g)). In the  $\alpha$ - $\text{In}_2\text{Se}_3$  ferroelectric diode, the polarization reversal in  $\alpha$ - $\text{In}_2\text{Se}_3$  changes the direction of the built-in electric field. The Schottky barrier height at the interfaces of the upper and lower sides of  $\alpha$ - $\text{In}_2\text{Se}_3$  changes significantly, leading to the switch of the conduction direction of the diode. Further studies on the  $I$ - $V$  characteristic of the ferroelectric diode under high DC bias are also performed. The  $I$ - $V$  curves are measured by sweeping the bias voltage from -2 to +2 V and then backward to -2 V. As shown in Fig. 4(e), under high DC bias with both positive and negative voltages, the device is at its "on" state due to the modification of Schottky barrier. The on/off ratio of the ferroelectric diode was found to be at the order of  $\sim 10^5$ .

A second typical example of the ferroelectric device application is the nonvolatile memory via the device so called FeFET, which is a kind of the three-terminal device by separating the reading operation in the conducting channel from the writing operation in and the ferroelectric gate. FeFETs are non-destructive with no requirement on ferroelectric film thickness. However, the thickness of ferroelectric used in conventional FeFET devices are usually of several hundred nanometers due to the constraint of Critical size effect. Therefore, relatively large operation gate voltage is always required. In contrast, 2D ferroelectrics will significantly scale down the dimensions of the device and meanwhile the voltage to flip the electric polarization could be lowered down dramatically, resulting a low-power consumption memory device.

Fig. 5 shows the schematic and optical image of a FeFET device based on graphene and ferroelectric  $\alpha$ - $\text{In}_2\text{Se}_3$ <sup>[29]</sup>. Atomically thin hexagonal boron nitride (hBN), monolayer or bilayer, was chosen as the buffer and insulating layer. The introduction of hBN layer not only improves the device interface properties, such as suppression of ion diffusion and leakage current<sup>[40, 41]</sup>, but also enhances the intrinsic conductivity of graphene by reducing the phonon and Coulomb scatterings. The thinnest thickness of the ferroelectric film in the device is 2.6 nm, which is roughly about the thickness of bilayer  $\alpha$ - $\text{In}_2\text{Se}_3$ . This thickness is much thinner than conventional ferroelectric layer. The resistance of graphene channel is controllable and retentive due to the electrostatic doping, which stems from the electric polarization of the ferroelectric  $\alpha$ - $\text{In}_2\text{Se}_3$ . As shown in Fig. 5(b), when sweeping the ferroelectric gate voltage cyclically from negative to positive and back to negative, the resistance of the graphene channel could be efficiently modulated with large and stable hysteresis. By applying the top-gate voltage, the electric dipoles in  $\alpha$ - $\text{In}_2\text{Se}_3$  are electrically polarized in the out-of-plane direction, either upward or downward. The dipoles would significantly dope graphene with different types of carriers via the induced screening charges, leading to the change of its Fermi level ( $E_F$ ) accompanied by the resistance modulation of the FeFET device. When the Fermi level is tuned to the Dirac point, the conducting

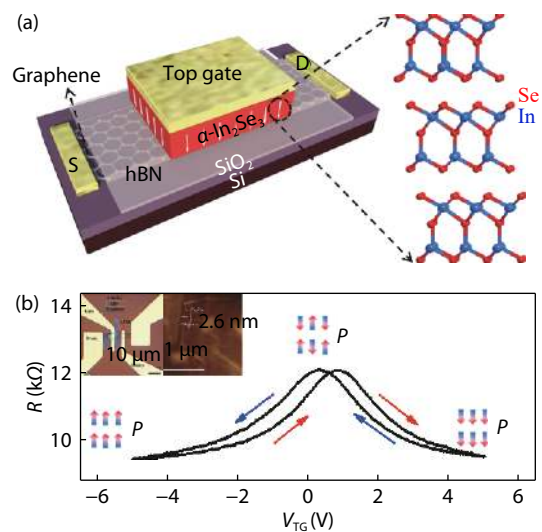


Fig. 5. (Color online) Structure and optical characterization of the 2D FeFET. (a) 3D schematic diagram of the FeFET. The FeFET is fabricated by vertically stacking graphene, hBN, and  $\alpha$ - $\text{In}_2\text{Se}_3$  thin layers in sequence. The white arrows indicate the direction of electric polarization. The zoomed area shows the crystal structure of ferroelectric  $\alpha$ - $\text{In}_2\text{Se}_3$ . (b) The hysteretic ferroelectric loop in 2D  $\alpha$ - $\text{In}_2\text{Se}_3$  based FeFET. The resistance follows a butterfly-like dependence on gate voltage. Inset shows the optical image and topography of the FeFET. The substrate is Si wafer with 300 nm fused  $\text{SiO}_2$  on top. The graphene, hBN, and ultrathin  $\alpha$ - $\text{In}_2\text{Se}_3$  are indicated by black, white, and red-dashed frames, respectively. From the AFM topography, the thinnest area of ultrathin  $\alpha$ - $\text{In}_2\text{Se}_3$  in the device is 2.6 nm. (Courtesy of Ref. [29])

graphene channel reaches its maximum resistance ( $R_{\text{Max}}$ ) state. Two  $R_{\text{Max}}$  states are found at different top gate voltages in the forward (from negative to positive) and backward (from positive to negative) gate voltage sweeping. The apparent differences of gate voltage at  $R_{\text{Max}}$  are due to the requirement of coercive electric field for domain reversion in ferroelectric  $\alpha$ - $\text{In}_2\text{Se}_3$ . However, even under  $\pm 5$  V gate bias, equivalent to an electrical field strength at the order of  $10^5$  V/cm in this device, the ferroelectric polarization in the top  $\alpha$ - $\text{In}_2\text{Se}_3$  thin layers does not get saturated. Moreover, it is necessary to point out that the observed hysteretic dependence of resistance on  $V_{\text{TG}}$  allowed us to explore the reversal processes of the electric dipoles in ferroelectric  $\alpha$ - $\text{In}_2\text{Se}_3$ .

## 5. Conclusions and outlooks

The vdW materials are promising for realizing 2D ferroelectricity which is the long-sought goal in conventional ferroelectrics. Recent progresses, especially the studies on ultra-thin ferroelectric  $\alpha$ - $\text{In}_2\text{Se}_3$ , have confirmed their practicability in device applications. They offer a versatile platform to study the ferroelectricity, domain physics, and ferroelectric device at nanometer scale. For  $\alpha$ - $\text{In}_2\text{Se}_3$ , due to its unique lattice structure, the in-plane and out-of-plane polarizations are inherently coupled, which provides a novel opportunity to control the out-of-plane ferroelectricity by in-plane electric field. However, one of the major bottlenecks for developing 2D ferroelectrics lies in the imperfect sample quality and uniformity. Large-scale ferroelectric thin-film synthesis techniques, such as molecular beam epitaxy (MBE) and chemical vapor depos-



ition (CVD), are highly desired for future practical device application.

## Acknowledgments

This work was supported by the National Key Research and Development Program of China (Grant Nos. 2017YFA0205004, 2018YFA03066004, and 2016YFA0301700), the National Natural Science Foundation of China (Grant Nos. 11674295 and 11774328), the Fundamental Research Funds for the Central Universities (Grant No. WK2340000082), Anhui Initiative in Quantum Information Technologies (Grant No. AHY170000), the USTC start-up funding and the China Government Youth 1000-Plan Talent Program.

## References

- [1] de Araujo C A P, Cuchiaro J D, McMillan L D, et al. Fatigue-free ferroelectric capacitors with platinum electrodes. *Nature*, 1995, 374(6523), 627
- [2] Choi T, Lee S, Choi Y J, et al. Switchable ferroelectric diode and photovoltaic effect in BiFeO<sub>3</sub>. *Science*, 2009, 324(5923), 63
- [3] Lu H, Lipatov A, Ryu S, et al. Ferroelectric tunnel junctions with graphene electrodes. *Nat Commun*, 2014, 5, 5518
- [4] Scott J F, Paz de Araujo C A. Ferroelectric memories. *Science*, 1989, 246(4936), 1400
- [5] Chu M W, Szafraniak I, Scholz R, et al. Impact of misfit dislocations on the polarization instability of epitaxial nanostructured ferroelectric perovskites. *Nat Mater*, 2004, 3(2), 87
- [6] Stengel M, Vanderbilt D, Spaldin N A. Enhancement of ferroelectricity at metal-oxide interfaces. *Nat Mater*, 2009, 8, 392
- [7] Lu H, Liu X, Burton J D, et al. Enhancement of ferroelectric polarization stability by interface engineering. *Adv Mater*, 2012, 24(9), 1209
- [8] Junquera J, Ghosez P. Critical thickness for ferroelectricity in perovskite ultrathin films. *Nature*, 2003, 422(6931), 506
- [9] Gao P, Zhang Z Y, Li M Q, et al. Possible absence of critical thickness and size effect in ultrathin perovskite ferroelectric films. *Nat Commun*, 2017, 8, 15549
- [10] Xi X X, Wang Z F, Zhao W W, et al. Ising pairing in superconducting NbSe<sub>2</sub> atomic layers. *Nat Phys*, 2015, 12, 139
- [11] Xi X X, Zhao L, Wang Z F, et al. Strongly enhanced charge-density-wave order in monolayer NbSe<sub>2</sub>. *Nature Nanotech*, 2015, 10, 765
- [12] Zeng H L, Dai J F, Yao W, et al. Valley polarization in MoS<sub>2</sub> monolayers by optical pumping. *Nat Nanotech*, 2012, 7, 490
- [13] Deng Y, Yu Y, Song Y, et al. Gate-tunable room-temperature ferromagnetism in two-dimensional Fe<sub>3</sub>GeTe<sub>2</sub>. *Nature*, 2018, 563(7729), 94
- [14] Geim A K, Novoselov K S. The rise of graphene. *Nat Mater*, 2007, 6, 183
- [15] Mak K F, Lee C G, Hone J, et al. Atomically thin MoS<sub>2</sub>: a new direct-gap semiconductor. *Phys Rev Lett*, 2010, 105(13), 136805
- [16] Zeng H L, Cui X D. An optical spectroscopic study on two-dimensional group-VI transition metal dichalcogenides. *Chem Soc Rev*, 2015, 44(9), 2629
- [17] Belianinov A, He Q, Dziaugys A, et al. CuInP<sub>2</sub>S<sub>6</sub> room temperature layered ferroelectric. *Nano Lett*, 2015, 15(6), 3808
- [18] Liu F C, You L, Seyler K L, et al. Room-temperature ferroelectricity in CuInP<sub>2</sub>S<sub>6</sub> ultrathin flakes. *Nat Commun*, 2016, 7, 12357
- [19] Chang K, Liu J W, Lin H C, et al. Discovery of robust in-plane ferroelectricity in atomic-thick SnTe. *Science*, 2016, 353(6296), 274
- [20] Ding W J, Zhu J B, Wang Z, et al. Prediction of intrinsic two-dimensional ferroelectrics in In<sub>2</sub>Se<sub>3</sub> and other III<sub>2</sub>-VI<sub>3</sub> van der Waals materials. *Nat Commun*, 2017, 8, 14956
- [21] Zhou Y, Wu D, Zhu Y H, et al. Out-of-plane piezoelectricity and ferroelectricity in layered  $\alpha$ -In<sub>2</sub>Se<sub>3</sub> nanoflakes. *Nano Lett*, 2017, 17(9), 5508
- [22] Cui C J, Hu W J, Yan X X, et al. Intercorrelated in-plane and out-of-plane ferroelectricity in ultrathin two-dimensional layered semiconductor In<sub>2</sub>Se<sub>3</sub>. *Nano Lett*, 2018, 18(2), 1253
- [23] Poh S M, Tan S J R, Wang H, et al. Molecular-beam epitaxy of two-dimensional In<sub>2</sub>Se<sub>3</sub> and its giant electroresistance switching in ferroresistive memory junction. *Nano Lett*, 2018, 18(10), 6340
- [24] Wan S Y, Li Y, Li W, et al. Room-temperature ferroelectricity and a switchable diode effect in two-dimensional  $\alpha$ -In<sub>2</sub>Se<sub>3</sub> thin layers. *Nanoscale*, 2018, 10(31), 14885
- [25] Xiao J, Zhu H, Wang Y, et al. Intrinsic two-dimensional ferroelectricity with dipole locking. *Phys Rev Lett*, 2018, 120(22), 227601
- [26] Xue F, Hu W, Lee K C, et al. Room-temperature ferroelectricity in hexagonally layered  $\alpha$ -In<sub>2</sub>Se<sub>3</sub> nanoflakes down to the monolayer limit. *Adv Funct Mater*, 2018, 0(0), 1803738
- [27] Xue F, Zhang J, Hu W, et al. Multidirection piezoelectricity in mono- and multilayered hexagonal  $\alpha$ -In<sub>2</sub>Se<sub>3</sub>. *ACS Nano*, 2018, 12(5), 4976
- [28] Zheng C, Yu L, Zhu L, et al. Room temperature in-plane ferroelectricity in van der Waals In<sub>2</sub>Se<sub>3</sub>. *Sci Adv*, 2018, 4(7), eaar7720
- [29] Wan S Y, Li Y, Li W, et al. Nonvolatile ferroelectric memory effect in ultrathin  $\alpha$ -In<sub>2</sub>Se<sub>3</sub>. *Adv Funct Mater*, 2018, 29, 1808606
- [30] Si M W, Gao S J, Qiu G, et al. A ferroelectric semiconductor field-effect transistor. arXiv: 1812.02933
- [31] Tao X, Gu Y. Crystalline-crystalline phase transformation in two-dimensional In<sub>2</sub>Se<sub>3</sub> thin layers. *Nano Lett*, 2013, 13(8), 3501
- [32] Wu D, Pak A J, Liu Y N, et al. Thickness-dependent dielectric constant of few-layer In<sub>2</sub>Se<sub>3</sub> nanoflakes. *Nano Lett*, 2015, 15(12), 8136
- [33] Zhou J D, Zeng Q S, Lv D H, et al. Controlled synthesis of high-quality monolayered  $\alpha$ -In<sub>2</sub>Se<sub>3</sub> via physical vapor deposition. *Nano Lett*, 2015, 15(10), 6400
- [34] Jacobs-Gedrim R B, Shanmugam M, Jain N, et al. Extraordinary photoresponse in two-dimensional In<sub>2</sub>Se<sub>3</sub> nanosheets. *ACS Nano*, 2014, 8(1), 514
- [35] Nilanthi B, Christopher R S, Emily F S, et al. Quantum confinement and photoresponsivity of  $\beta$ -In<sub>2</sub>Se<sub>3</sub> nanosheets grown by physical vapour transport. *2D Mater*, 2016, 3(2), 025030
- [36] Choi M S, Cheong B K, Ra C H, et al. Electrically driven reversible phase changes in layered In<sub>2</sub>Se<sub>3</sub> crystalline film. *Adv Mater*, 2017, 29(42), 1703568
- [37] Lewandowska R, Bacewicz R, Filipowicz J, et al. Raman scattering in  $\alpha$ -In<sub>2</sub>Se<sub>3</sub> crystals. *Mater Res Bull*, 2001, 36(15), 2577
- [38] Debbichi L, Eriksson O, Lebegue S. Two-dimensional indium selenides compounds: an ab initio study. *J Phys Chem Lett*, 2015, 6(15), 3098
- [39] Zhou S, Tao X, Gu Y. Thickness-dependent thermal conductivity of suspended two-dimensional single-crystal In<sub>2</sub>Se<sub>3</sub> layers grown by chemical vapor deposition. *J Phys Chem C*, 2016, 120(9), 4753
- [40] Eisuke T, Kojiro O, Hiroshi I. Low voltage operation of nonvolatile metal-ferroelectric-metal-insulator-semiconductor (MFIS) field-effect-transistors (FETs) using Pt/SrBi<sub>2</sub>Ta<sub>2</sub>O<sub>9</sub>/Pt/SrTa<sub>2</sub>O<sub>6</sub>/SiON/Si structures. *Jpn J Appl Phys*, 2001, 40(4S), 2917
- [41] Eisuke T, Gen F, Hiroshi I. Electrical properties of metal-ferroelectric-insulator-semiconductor (MFIS) and metal-ferroelectric-metal-insulator-semiconductor (MFIS)-FETs using ferroelectric SrBi<sub>2</sub>Ta<sub>2</sub>O<sub>9</sub> film and SrTa<sub>2</sub>O<sub>6</sub>/SiON buffer layer. *Jpn J Appl Phys*, 2000, 39(4S), 2125